Competing Ion Decomposition Channels in Matrix-Assisted Laser Desorption Ionization

Guanghong Luo, Ioan Marginean,† Louise Ye, and Akos Vertes*

Department of Chemistry, The George Washington University, Washington, D.C. 20052

Received: November 9, 2007; Revised Manuscript Received: March 5, 2008

We gauged the internal energy transfer for two dissociative ion decomposition channels in matrix-assisted laser desorption ionization (MALDI) using the benzyltriphenylphosphonium (BTP) thermometer ion $[PhCH_2PPh_3]^+$. Common MALDI matrixes [α-cyano-4-hydroxycinnamic acid (CHCA), 3,5-dimethoxy-4-hydroxycinnamic acid (sinapinic acid, SA), and 2,5-dihydroxycinnamic acid (DHB)] were studied with nitrogen laser (4 ns pulse length) and mode-locked $3 \times \omega$ Nd:YAG laser (22 ps pulse length) excitation. Despite the higher fluence required to initiate fragmentation, BTP ions indicated lower internal energy transfer with the picosecond laser in all three matrixes. These differences can be rationalized in terms of phase explosion induced by the nanosecond laser vs a stress-confinement-driven desorption mechanism for the picosecond laser. For the two ion production channels of the BTP thermometer ion, breaking a single bond can result in the formation of benzyl/tropylium ions, F1, or triphenylphosphine ions, F2. In SA and DHB, as well as in CHCA at low fluence levels, the efficiency of these channels (expressed by the branching ratio I_{F1}/I_{F2}) is moderately in favor of producing tropylium ions, $1 < I_{F1}/I_{F2} < 6$. As the laser fluence is increased, for CHCA, there is a dramatic shift in favor of the tropylium ion production, with $I_{F1}/I_{F2} \approx 30$ for the nanosecond and the picosecond laser, respectively. This change is correlated with the sudden increase in the BTP internal energies in CHCA in the same laser fluence range. The large changes observed in internal energy deposition for CHCA with laser fluence can account for its ability to induce fragmentation in peptides more readily than SA and DHB.

Introduction

The fragmentation of metastable ions in matrix-assisted laser desorption/ionization (MALDI) is often used in structural studies of biopolymers. In these so-called post-source decay experiments, as well as in collision activated dissociation (CAD), the primary factor that governs the fragmentation is the internal energy of the ions.[1–13] Laser desorption from nanoparticles and nanostructures creates ions with more uniform internal energies and, as a result, with fragmentation patters that are less dependent on the laser fluence.[14–16] When fragmentation is enhanced by CAD, different peptide−ion fragmentation channels can be activated as the laser fluence is changed.[17,18]

As in MALDI, the direct absorption of laser energy by the analyte is typically negligible, the excess internal energy is a consequence of energy transfer from the matrix. The energy transfer between matrix and analyte is a combination of collisional transfer[19,20] and transfer via chemical reactions (e.g., proton transfer). It is believed that proton transfer deposits a relatively small amount of energy into the analyte, resulting only in weak fragmentation.[21–24] Several models, for example, the bottleneck model[25,26] and the explosive boiling model,[27] have been employed to rationalize the limited collisional energy transfer between matrix and analyte in MALDI. Others, such as the hydrodynamic model,[28] emphasized the stabilizing effect of expansion cooling in the laser plume.

Matrix ionization and fragmentation can be explained by exciton pooling[29] combined with ladder climbing and switching.[30–32] The model based on ladder climbing and switching explains the ionization and fragmentation of molecules during multiphoton ionization as a result of competitive pathways. In the ladder-climbing mode, the pumping rate is usually very high, and the molecule is consecutively excited to its ionization potential. At lower pumping rate, the molecule may fragment because a competing reaction channel is activated (ladder switching) before the energy of excitation reaches the ionization potential. This model is especially useful in explaining the results obtained in MALDI with different laser pulse lengths.[32]

In the case of a single unimolecular decomposition reaction, the molecular ion fragmentation can be quantified as the survival yield, and the RRKM theory can be used to extract the internal energy content of the fragmenting ion.[6] Recently, the internal energy transfer in MALDI was probed using benzyl-substituted benzylpyridinium (BP = $[RPhCH_2Pyr]^+$) salts as thermometer ions.[10–13] Their simple structure and the single fragmentation channel make these species ideal candidates for RRKM analysis. Because these analytes are present already in the solid phase as preformed ions (i.e., no ionization is needed), they can be used to follow energy transfer in the desorption process alone. For analytes that require an ionization step (for example, most peptides are ionized through proton transfer), the two forms of energy transfer cannot be separated.

Research on glycoproteins,[33] oligodeoxynucleotides,[21] and proteins[34] indicated that α-cyano-4-hydroxycinnamic acid (CHCA) was a hot matrix, triggering more analyte fragmentation, whereas 2,5-dihydroxycinnamic acid (DHB) was a cold matrix, inducing less fragmentation. Earlier work on a series of BP salts[10,12,13] indicated the opposite trend. On the basis of the mean values of analyte internal energy, CHCA, 3,5-dimethoxy-4-hydroxycinnamic acid (sinapinic acid, SA), and DHB were shown to be cool, intermediate, and hot matrixes, respectively. The explanation for this apparent contradiction can be two-fold. First,

* Corresponding author. Address: 725 21st Street, N.W., Washington, DC 20052. Phone: (202) 994-2717. Fax: (202) 994-5873, e-mail vertes@gwu.edu.

† Current address: Environmental Molecular Science Laboratory, Pacific Northwest National Laboratory, P.O. Box 999, Richland, WA 99354.

10.1021/jp710726c CCC: $40.75
Published on Web 05/20/2008

SCHEME 1

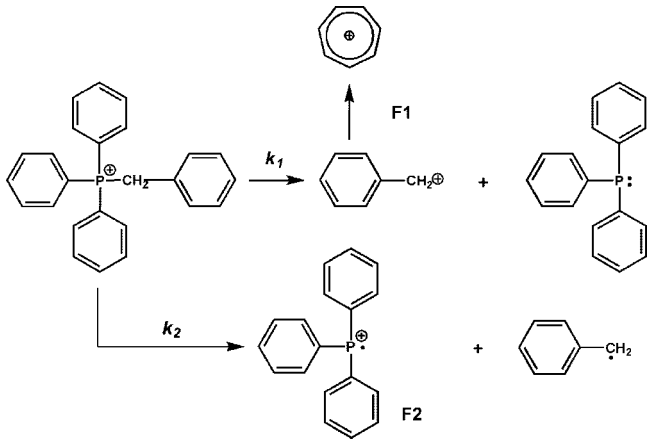

peptide−ionization in MALDI requires protonation, whereas the BP ions are preformed already in the solid phase. Second, it has been hypothesized that the fluence dependence of energy deposition exhibited a steeper rise in CHCA, resulting in a crossover in energy deposition order for the three matrixes at elevated fluences.[10] This hypothesis, however, was never tested due to the narrow fluence range available for SY experiments with BP ions.

Pump−probe experiments with split laser pulses of 30 ps length evidenced that the initial matrix ionization in the MALDI plume had a time scale of less than 2 ns.[35] Fluid dynamics modeling[28] and molecular dynamics simulations[36,37] showed that the desorption process started less than a nanosecond after the onset of the laser pulse. Plume expansion studies indicated an initial plume velocity of 1000 m/s and a desorption time scale of tens of picoseconds.[38] A phase transition was estimated to take place ~60 ps after the onset of laser heating.[37]

Comparing excitation on nanosecond and picosecond timescales in MALDI promises to provide information on desorption mechanisms (thermal vs stress confinement[27]) and on the primary ionization of the matrix.[32] A longer laser pulse (e.g., 4 ns for the nitrogen laser) interacts not only with the solid lattice but also with the expanding plume. This suggests that choosing laser pulse lengths shorter and longer than ~60 ps may enable us to distinguish the laser−solid and laser−plume interactions. In this study, two lasers, a nitrogen laser with a 4 ns pulse length and a mode-locked 3 × ω Nd:YAG laser with a 22 ps pulse length, were used to explore the relative significance of these processes in internal energy transfer.

Fragmentation of peptides and proteins in MALDI is the basis for sequencing and structure determination. In qualitative in-source decay experiments, the peptide backbone fragmentation channels were observed to depend on the laser fluence and on matrix material but not on the laser pulse length (700 ps versus 5 ns).[39–41] Recently, we showed that a nanosecond laser produced more matrix fragmentation at a lower fluence threshold as well as higher analyte ion yields than a picosecond laser.[32] Here, we report on experiments using different pulse lengths to explore internal energy transfer for the benzyltriphenylphosphonium (BTP = $[PhCH_2PPh_3]^+$) thermometer ion that possesses two competing charge partitioning pathways. The two channels for the BTP ions are presented in Scheme 1. This system can be viewed as a simple model to explore the effect of the matrix, laser fluence, and laser pulse length on the product ion distributions in MALDI. Using BTP thermometer ions also enabled us to study survival yields in a much wider fluence range than we could with BP ions.

Experimental Section

Materials, Lasers, and Mass Spectrometry. Because the experimental setup and procedures have been discussed in detail in a previous publication,[10] here we focus on only the differences. BTP chloride (99% purity, Sigma-Aldrich, Allentown, PA) was used as the analyte in three common MALDI matrixes: CHCA, SA, and DHB. A nitrogen laser (VSL-337ND, Laser Science Inc., Newton, MA), at 337 nm wavelength with 4 ns pulse length and 95 μm focal diameter, and a mode-locked 3 × ω Nd:YAG laser (PL2143, EKSPLA, Vilnius, Lithuania), at 355 nm wavelength with 22 ps pulse length and 55 μm focal diameter, were triggered at 2 Hz. A low-pass optical filter was implemented to reject the possible residue from the second harmonic (532 nm) component in the output of the 3 × ω Nd:YAG laser. The home-built linear time-of-flight mass spectrometer was operated at 25 kV accelerating voltage.

Survival Yields and Branching Ratios. The BTP and the individual matrix solutions were mixed to produce a matrix-to-analyte ratio of 20 000. Spectra were collected with laser fluence values within a range of 1.0−1.3 times the fragmentation threshold and averaged over the surface area. Data processing was described previously.[10] The analyte ion current peaks corresponding to the quasimolecular and fragment ions were integrated in time, and the survival yields were calculated as $SY = \Sigma I_M/(\Sigma I_M + \Sigma I_F)$, where I_M ($M^+ = [PhCH_2PPh_3]^+$) and I_F ($F1^+ = [PhCH_2]^+$ and $F2^+ = [PPh_3]^{+\bullet}$) are the abundances of the quasimolecular and fragment ions, respectively. To assess the relative importance of the two dissociative ion production channels, the branching ratios for the fragment ions $[PhCH_2]^+$ and $[PPh_3]^{+\bullet}$, $BR = I_{F1}/I_{F2}$, were also evaluated.

Results and Discussion

The yields of the BTP thermometer ion were recorded in MALDI experiments as a function of laser fluence. Although little or no fragmentation was observed at low fluence values, fragment ions appeared above a certain threshold. Figure 1 presents the mass spectra of the BTP salt desorbed from the DHB matrix with the two lasers at a fluence slightly above the fragmentation threshold. In addition to the matrix-related signal, the spectra contain peaks corresponding to the molecular, M^+, (m/z 353) and the fragment ions, $F1^+ = [PhCH_2]^+$ (m/z 91) and $F2^+ = [PPh_3]^{+\bullet}$ (m/z 262), of BTP. Both fragment ions were formed as the result of a single bond cleavage in the molecular ion with the positive charge distributed between the two fragments.

The influence of the laser pulse length on the ionization can be surmised by visually comparing the MALDI spectra. Despite the required higher fluence, when using the picosecond laser, less matrix fragmentation can be observed (compare panels a and b). In panel a, the intensity ratio of the matrix molecular ion to its fragment exhibiting an OH loss is ~2, whereas in panel b, the corresponding ratio is ~0.5. Similar to the matrix ions, the thermometer ion shows more prevalent fragmentation with the nanosecond laser (b) than with the picosecond laser (a). The survival yields of the BTP molecular ion in Figure 1a and b are ~0.87 and ~0.73, respectively, indicating that more fragmentation is induced by the nanosecond laser.

To study the relationship between the survival yield and the different ionization pathways, the ion yields of the intact $[PhCH_2PPh_3]^+$ cations and their fragments, the benzyl/tropylium ion, $[PhCH_2]^+$ and the triphenylphosphine ion, $[PPh_3]^{+\bullet}$, were recorded as a function of the laser fluence., Although in lieu of thermochemical data (e.g., critical energies) we cannot translate the observed survival yield values into actual internal energies,

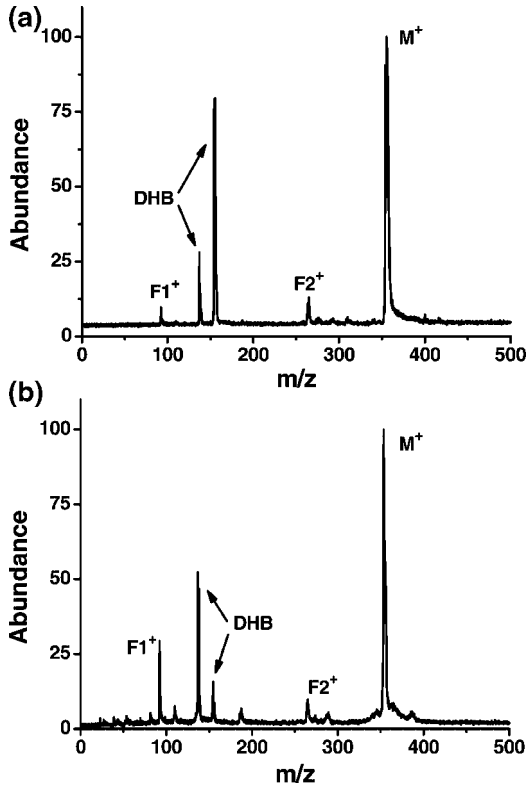

Figure 1. Mass spectra of BTP salt desorbed from DHB with (a) picosecond and (b) nanosecond lasers. The molecular ion, M^+, decomposes through two competing fragmentation channels, producing $F1^+$ and $F2^+$ fragment ions. The survival yields of the BTP molecular ion in parts a and b are ~0.87 and ~0.73, respectively, indicating that more fragmentation is induced by the nanosecond laser.

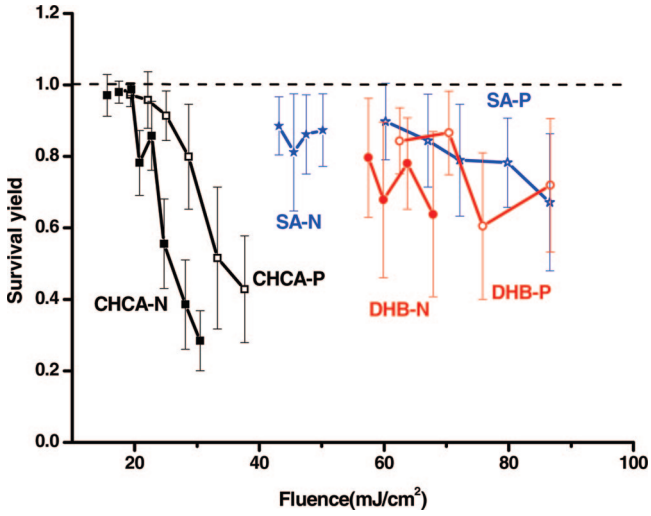

Figure 2. Survival yields for $[PhCH_2PPh_3]^+$ molecular ions desorbed from CHCA (black), SA (blue), and DHB (red) matrixes with nanosecond (solid symbols) and picosecond (hollow symbols) lasers.

due to the monotonic nature of $k_{RRKM}(E)$ curves, we can still use the survival yields to monitor the energy content of the BTP ions. Previously, $[PhCH_2PPh_3]^+$ had been used as a thermometer ion in a qualitative sense to demonstrate the different thermal load an analyte experiences in direct and in matrix-assisted laser desorption.[3]

Figure 2 shows the survival yield of the $[PhCH_2PPh_3]^+$ molecular ion in the three different matrixes, CHCA, SA, and DHB, as a function of laser fluence in the MALDI experiment. Close to the threshold (i.e., at 1.1−1.3×), intact $[PhCH_2PPh_3]^+$ ion production from CHCA proceeded with the highest yield for both lasers. From SA and DHB, the desorbed molecular ions showed reduced survival yields. This is similar to our earlier findings for the BP ions and indicates that close to the threshold fluence, CHCA produces the lowest internal energy transfer of the three matrixes.[10]

Analogous to the BP ions in ref 13, with the picosecond laser, higher fluence was required to detect the analyte ions than with the nanosecond laser, although the fluence gap between the two lasers was narrower. For CHCA and DHB, there was an overlap in the fluence range for the nanosecond and the picosecond lasers. In the range where both lasers could be used, the ion production with the picosecond laser invariably resulted in higher survival yields, that is, the picosecond laser induced less energy deposition into the $[PhCH_2PPh_3]^+$ ions.

When compared to the BP ions, BTP as a thermometer ion offered additional insight. In the CHCA matrix, the experiments were extended to relatively high fluence levels, that is, to ~2 times the fragmentation threshold. At the elevated fluence values for CHCA, Figure 2 shows a dramatic drop in survival yields for both the nanosecond and the picosecond laser. The uniquely broad range of survival yields for the $[PhCH_2PPh_3]^+$ ions, from close to 100% to less than 30%, reveals a special feature of the CHCA matrix. Whereas at low laser fluences, it produces more intact molecular ions than SA or DHB (i.e., it is "cooler"), as the laser fluence increases, CHCA quickly becomes "hotter"; that is, it produces more analyte fragments than the other two matrixes.

This observation helps to explain an apparent contradiction in the literature. In MALDI experiments for glycoproteins,[33] oligodeoxynucleotides,[21] and proteins,[34] CHCA was claimed to be a "hot" matrix, as compared to SA and DHB, due to the increased fragmentation it induced in these analytes. In our earlier report on fragmentation of preformed BP ions, we established the opposite trend.[10] This discrepancy was rationalized by separating internal energy transfer due to the desorption step and as a result of ionization (e.g., proton transfer). Whereas in MALDI, peptides, proteins, and nucleotides require ionization, the thermometer ions (both BP and BTP) are preformed already in the solid phase. Thus, they report only the energy transfer associated with the desorption step. The results in Figure 2 draw the attention to the effect of the laser fluence on the energy transfer in MALDI. For CHCA, the survival yield drops by a factor of 4 with increasing fluence, whereas for SA and DHB, no such dramatic decline can be observed. Thus, the different matrixes not only induce a different amount of energy transfer at the threshold fluence ("hot" vs "cold") but also have a different ability to impart additional internal energy as the laser fluence increases.

Rapid energy deposition with a 22 ps pulse apparently results in higher survival yield, that is, less internal energy, in the BTP ion. Although a similar phenomenon was observed in the primary ionization of DHB,[32] in that case, the enhanced molecular ion yield for 22 ps excitation was due to the shift from ladder switching to ladder climbing in the strongly absorbing matrix material. Due to its negligible light absorption at the laser wavelength, this explanation does not work for the BTP ion. Instead, the higher survival yield can be explained by the fundamentally different plume formation mechanism for short laser pulses. If the laser pulse length is comparable to the heat conduction and heat dissipation times (typically on the nanosecond scale), the MALDI process can be described by a phase explosion due to the thermal confinement,[27,42] and efficient

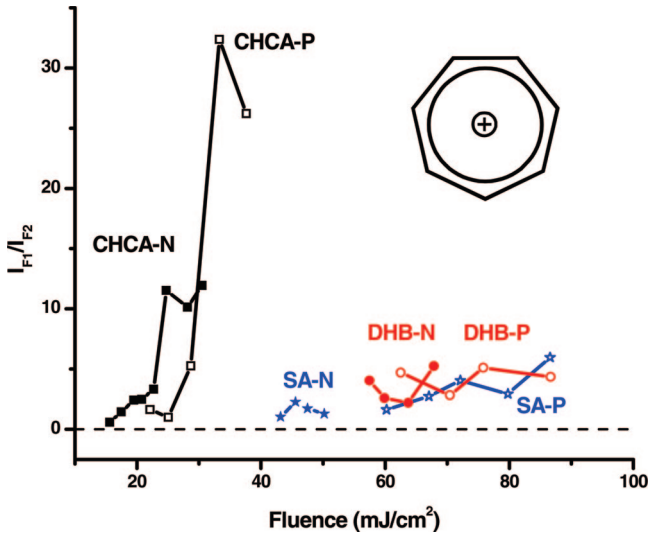

Figure 3. Branching ratio for tropylium, $F1^+ = [PhCH_2]^+$, and triphenylphosphine, $F2^+ = [PPh_3]^{+\bullet}$, fragment ions produced from $[PhCH_2PPh_3]^+$ molecular ions in desorption with nanosecond (solid symbols) and picosecond (hollow symbols) lasers from CHCA (black), SA (blue), and DHB (red) matrixes.

energy transfer is expected in the plume. Laser pulses shorter than the time required for heat dissipation, however, are associated with the stress confinement regime of ablation. In this regime, larger clusters are produced in a higher proportion, and the energy transfer to the thermometer ions is less efficient. This is manifested in a higher survival yield at the same fluence.

Due to the presence of the two ion decomposition channels, the fragmentation of $[PhCH_2PPh_3]^+$ can result in $[PhCH_2]^+$ and $[PPh_3]^{+\bullet}$ ions. To see how the increased energy deposition affected these two channels, we followed the corresponding branching ratio, I_{F1}/I_{F2}, as a function of the fluence (see Figure 3). In SA and DHB, these ratios fairly uniformly fall in the range of 1−6 and do not depend on the fluence significantly. In CHCA, however, the flat response in the low fluence range is followed by a dramatic increase to ∼10 and ∼30 for the nanosecond and the picosecond laser, respectively. The fluence where this major change takes place coincides with the breakdown fluence for the survival yield curves, that is, where the internal energy of the $[PhCH_2PPh_3]^+$ ions suddenly increases. The coincidence indicates that the increase in the internal energy of the molecular ion results in more fragmentation into benzyl/tropylium ions while the formation of triphenylphosphine ions remains close to the original level.

Branching ratios of competing reaction channels have been extensively studied (see, for example, ref 43). In the framework of the Rice−Ramsperger−Kassel−Marcus (RRKM) theory for unimolecular decomposition, the branching ratio can be expressed as:

$$\mathrm{BR} = \frac{\int \frac{G_1(E)}{G_1(E)+G_2(E)} P(E)\,\mathrm{d}E}{\int \frac{G_2(E)}{G_1(E)+G_2(E)} P(E)\,\mathrm{d}E} \qquad (1)$$

where $P(E)$ is the normalized internal energy distribution of the decomposing ion, and $G_1(E)$ and $G_2(E)$ are the total numbers of states between the transition state energies and the E energy level. Thus, for these reactions, the branching ratio depends on the internal energy distribution of the decomposing ion, the activation energies of the two reactions, and the number of states for the transition state. Among these, the matrix environment can primarily influence the internal energy distribution. Indeed, comparing Figures 2 and 3, we find that the branching ratio and the survival yield (an indicator of internal energy) exhibit correlated response to changes in laser fluence.

A further feature of the branching ratios in Figure 3 is that above the fluence threshold for the dominance of the F_1 channel, the picosecond laser produces 3 times more skewed I_{F1}/I_{F2} ratios. Whereas for the nanosecond laser this value is ∼10, for the picosecond laser, $I_{F1}/I_{F2} \approx 30$. The enhanced ability of the picosecond laser to favor one reaction channel over the other compared to the nanosecond laser does not lend itself to simple explanation. From the corresponding survival yield curves (Figure 2), it seems that the desorption process with the picosecond laser requires slightly higher fluence, and it imparts less internal energy, yet the product branching ratio is more lopsided. Thus, this effect cannot be explained on the basis of differences in internal energy alone, and a feasible explanation requires further studies.

Conclusions

Using preformed BTP ions as probes for internal energy transfer in MALDI, we demonstrated that for SA and DHB matrixes, the energy content of the ions after the desorption event is only slightly dependent on the laser pulse length. In CHCA, the nanosecond laser excitation resulted in significantly lower survival yields than the picosecond laser pulses. The fluence dependence of the survival yield exhibited a steeper drop in CHCA than in the other two matrixes. This resulted in a crossover in energy deposition order for the three matrixes at elevated fluences; that is, whereas at low fluences, CHCE deposits less energy into the BTP ion than SA and DHB, at higher fluences, the opposite is true.

Competition between the ion decomposition channels in MALDI is critical for peptide sequencing and protein analysis. Following the branching ratios for the $[PhCH_2PPh_3]^+$ ion with two alternative fragmentation channels offers a way to correlate the competing decomposition pathways with the internal energy content imparted by the MALDI process. Our experiments show that the choice of matrix, the laser fluence, and to a lesser degree, the pulse duration affect the branching ratio. Because this study focuses on preformed ions, the role of the ionization in product internal energies is not reflected. To understand peptide fragmentation in MALDI, the role of ionization in internal energy transfer for systems with multiple fragmentation channels also needs to be explored.

Acknowledgment. The authors are grateful for the financial support from the Chemical Sciences, Geosciences and Biosciences Division within the Office of Basic Energy Sciences of the U.S. Department of Energy (DE-FG02-01ER15129) and from the George Washington University Research Enhancement Fund (GWU-REF). Support from the Department of Energy does not constitute an endorsement of the views expressed in the article. Technical assistance with the Nd:YAG laser by Y. Chen is greatly appreciated.

References and Notes

(1) Huth-Fehre, T.; Becker, C. H. *Rapid Commun. Mass Spectrom.* **1991**, *5*, 378–382.

(2) Spengler, B.; Kirsch, D.; Kaufmann, R.; Jaeger, E. *Rapid Commun. Mass Spectrom.* **1992**, *6*, 105–108.

(3) Claereboudt, J.; Claeys, M.; Geise, H.; Gijbels, R.; Vertes, A. *J. Am. Soc. Mass Spectrom.* **1993**, *4*, 798–812.

(4) Mowry, C. D.; Johnston, M. V. *J. Phys. Chem.* **1994**, *98*, 1904–1909.

(5) Kinsel, G. R.; Preston, L. M.; Russell, D. H. *Biol. Mass Spectrom.* **1994**, *23*, 205–211.

(6) Vekey, K. *J. Mass Spectrom.* **1996**, *31*, 445–463.

(7) Krutchinsky, A. N.; Loboda, A. V.; Spicer, V. L.; Dworschak, R.; Ens, W.; Standing, K. G. *Rapid Commun. Mass Spectrom.* **1998**, *12*, 508–518.

(8) Stevenson, E.; Breuker, K.; Zenobi, R. *J. Mass Spectrom.* **2000**, *35*, 1035–1041.

(9) Medzihradszky, K. F.; Campbell, J. M.; Baldwin, M. A.; Falick, A. M.; Juhasz, P.; Vestal, M. L.; Burlingame, A. L. *Anal. Chem.* **2000**, *72*, 552–558.

(10) Luo, G. H.; Marginean, I.; Vertes, A. *Anal. Chem.* **2002**, *74*, 6185–6190.

(11) Greisch, J. F.; Gabelica, V.; Remacle, F.; De Pauw, E. *Rapid Commun. Mass Spectrom.* **2003**, *17*, 1847–1854.

(12) Gabelica, V.; Schulz, E.; Karas, M. *J. Mass Spectrom.* **2004**, *39*, 579–593.

(13) Vertes, A.; Luo, G. H.; Ye, L.; Chen, Y.; Marginean, I. *Appl. Phys. A: Mater. Sci. Process.* **2004**, *79*, 823–825.

(14) Luo, G. H.; Chen, Y.; Daniels, H.; Dubrow, R.; Vertes, A. *J. Phys. Chem. B* **2006**, *110*, 13381–13386.

(15) Luo, G. H.; Chen, Y.; Siuzdak, G.; Vertes, A. *J. Phys. Chem. B* **2005**, *109*, 24450–24456.

(16) Chen, Y.; Vertes, A. *Anal. Chem.* **2006**, *78*, 5835–5844.

(17) Campbell, J. M.; Vestal, M. L.; Blank, P. S.; Stein, S. E.; Epstein, J. A.; Yergey, A. L. *J. Am. Soc. Mass Spectrom.* **2007**, *18*, 607–616.

(18) Khatun, J.; Ramkissoon, K.; Giddings, M. C. *Anal. Chem.* **2007**, *79*, 3032–3040.

(19) Westman, A.; Demirev, P.; Huth-Fehre, T.; Bielawski, J.; Sundqvist, B. U. R. *Int. J. Mass Spectrom. Ion Processes* **1994**, *130*, 107–115.

(20) Moneti, G.; Francese, S.; Mastrobuoni, G.; Pieraccini, G.; Seraglia, R.; Valitutti, G.; Traldi, P. *J. Mass Spectrom.* **2007**, *42*, 117–126.

(21) Zhu, L.; Parr, G. R.; Fitzgerald, M. C.; Nelson, C. M.; Smith, L. M. *J. Am. Chem. Soc.* **1995**, *117*, 6048–6056.

(22) Zhu, Y. F.; Lee, K. L.; Tang, K.; Allman, S. L.; Taranenko, N. I.; Chen, C. H. *Rapid Commun. Mass Spectrom.* **1995**, *9*, 1315–1320.

(23) Tang, W.; Krause, J.; Zhu, L.; Smith, L. M. *Int. J. Mass Spectrom.* **1997**, *169*, 301–311.

(24) Stimson, E.; Truong, O.; Richter, W. J.; Waterfield, M. D.; Burlingame, A. L. *Int. J. Mass Spectrom.* **1997**, *169*, 231–240.

(25) Vertes, A.; Gijbels, R.; Levine, R. D. *Rapid Commun. Mass Spectrom.* **1990**, *4*, 228–233.

(26) Vertes, A.; Levine, R. D. *Chem. Phys. Lett.* **1990**, *171*, 284–290.

(27) Zhigilei, L. V.; Garrison, B. J. *J. Appl. Phys.* **2000**, *88*, 1281–1298.

(28) Vertes, A.; Irinyi, G.; Gijbels, R. *Anal. Chem.* **1993**, *65*, 2389–2393.

(29) Karbach, V.; Knochenmuss, R. *Rapid Commun. Mass Spectrom.* **1998**, *12*, 968–974.

(30) Szaflarski, D. M.; Elsayed, M. A. *J. Phys. Chem.* **1988**, *92*, 2234–2239.

(31) Weinkauf, R.; Aicher, P.; Wesley, G.; Grotemeyer, J.; Schlag, E. W. *J. Phys. Chem.* **1994**, *98*, 8381–8391.

(32) Chen, Y.; Vertes, A. *J. Phys. Chem. A* **2003**, *107*, 9754–9761.

(33) Karas, M.; Bahr, U.; Strupat, K.; Hillenkamp, F.; Tsarbopoulos, A.; Pramanik, B. N. *Anal. Chem.* **1995**, *67*, 675–679.

(34) Spengler, B.; Kirsch, D.; Kaufmann, R. *J. Phys. Chem.* **1992**, *96*, 9678–9684.

(35) Knochenmuss, R.; Vertes, A. *J. Phys. Chem. B* **2000**, *104*, 5406–5410.

(36) Zhigilei, L. V.; Garrison, B. J. *Appl. Phys. A: Mater. Sci. Process.* **1999**, *69*, S75−S80.

(37) Sadeghi, M.; Wu, X. W.; Vertes, A. *J. Phys. Chem. B* **2001**, *105*, 2578–2587.

(38) Puretzky, A. A.; Geohegan, D. B.; Hurst, G. B.; Buchanan, M. V.; Luk'yanchuk, B. S. *Phys. Rev. Lett.* **1999**, *83*, 444–447.

(39) Brown, R. S.; Feng, J.; Reiber, D. C. *Int. J. Mass Spectrom. Ion Processes* **1997**, *169*, 1–18.

(40) Brown, R. S.; Lennon, J. J. *Anal. Chem.* **1995**, *67*, 1998–2003.

(41) Brown, R. S.; Carr, B. L.; Lennon, J. J. *J. Am. Soc. Mass Spectrom.* **1996**, *7*, 225–232.

(42) Chen, Z.; Bogaerts, A.; Vertes, A. *Appl. Phys. Lett.* **2006**, *89*, 041503.

(43) Craig, S. L.; Zhong, M. L.; Choo, B.; Brauman, J. I. *J. Phys. Chem. A* **1997**, *101*, 19–24.

JP710726C